Patterns of thaumarchaeal gene expression in culture and diverse marine environments

Authors:
Paul Carini[1,3], Christopher L. Dupont[2], Alyson E. Santoro[1,4]

[1]Horn Point Laboratory, University of Maryland Center for Environmental Science, Cambridge, MD 21613
[2]J. Craig Venter Institute, San Diego, CA 92037
[3]Present Address: Department of Soil, Water and Environmental Science, University of Arizona, Tucson, AZ 85721
[4]Present address: Department of Ecology, Evolution, and Marine Biology, University of California, Santa Barbara, CA 93106

Keywords: Thaumarchaea, nitrification, metatranscriptome, NirK, nitrogen cycling

Corresponding Author: Alyson Santoro (alyson.santoro@lifesci.ucsb.edu)

Abstract
Thaumarchaea are ubiquitous in marine habitats where they participate in carbon and nitrogen cycling. Although metatranscriptomes suggest thaumarchaea are active microbes in marine waters, we understand little about how thaumarchaeal gene expression patterns relate to substrate utilization and activity. Here, we report the global transcriptional response of the marine ammonia-oxidizing thaumarchaeon '*Candidatus* Nitrosopelagicus brevis' str. CN25 to ammonia limitation using RNA-Seq. We further describe the genome and transcriptome of *Ca*. N. brevis str. U25, a new strain capable of urea utilization. Ammonia limitation in CN25 resulted in reduced expression of transcripts coding for ammonia oxidation proteins, and increased expression of a gene coding an Hsp20-like chaperone. Despite significantly different transcript abundances across treatments, two ammonia monooxygenase subunits (*amoAB*), a nitrite reductase (*nirK*), and both ammonium transporter genes were always among the most abundant transcripts, regardless of growth state. *Ca*. N. brevis str. U25 cells expressed a urea transporter 139-fold more than the urease catalytic subunit *ureC*. Gene co-expression networks derived from culture transcriptomes and ten thaumarchaea-enriched metatranscriptomes

revealed a high degree of correlated gene expression across disparate environmental conditions and identified a module of genes, including *amoABC* and *nirK*, that we hypothesize to represent the core ammonia oxidation machinery.

Originality-Significance Statement:

Discovering gene function in fastidious or uncultivated lineages remains one of the biggest challenges in environmental microbiology. Here, we use an approach that combines controlled laboratory experiments with *in situ* transcript abundance data from the environment to identify genes that share similar transcription patterns in marine ammonia-oxidizing thaumarchaea. These findings demonstrate how transcriptomes from microbial cultures can be used together with complex environmental samples to identify suites of co-expressed genes that are otherwise enigmatic and provide new insights into the mechanism of ammonia oxidation. Our results add to the growing body of literature showing that relatively small changes in transcript abundance are linked to large changes in growth in organisms with reduced genomes, suggesting they have limited capacity for metabolic regulation or that they rely on mechanisms other than transcriptional regulation to deal with a fluctuating environment.

Introduction:

Ammonia-oxidizing thaumarchaea are ubiquitous and abundant in the oceans, accounting for >30% of all cells below the thermocline (Karner *et al.*, 2001; Schattenhofer *et al.*, 2009) and are integral organisms in oxygen minimum zones (Francis *et al.*, 2005; Coolen *et al.*, 2007; Lam *et al.*, 2009; Pitcher *et al.*, 2011; Stewart *et al.*, 2012; Beman *et al.*, 2012). In many marine environments, thaumarchaeal transcripts are among the most abundant that can be mapped to available prokaryotic genomes (Hollibaugh *et al.*, 2011; Baker *et al.*, 2012; Stewart *et al.*, 2012; Gifford *et al.*, 2013). In these environments, the most frequently detected thaumarchaeal transcripts encode for proteins involved in ammonia oxidation and acquisition, including ammonia monooxygenase subunits (*amoABC*), ammonium transporters (*amtB*), a putative Cu-containing nitrite reductase (*nirK*), and structural cellular components (for example, S-layer proteins (Nakagawa and Stahl, 2013)). In addition to dissolved ammonia, some ammonia-oxidizing archaea utilize ammonia derived from urease-

77 catalyzed urea hydrolysis as a chemolithoautotrophic growth substrate (Qin
78 *et al.*, 2014; Bayer *et al.*, 2015) and urease genes and transcripts believed
79 to be of thaumarchaeal origin have been detected in marine environments
80 (Shi *et al.*, 2010; Alonso-Sáez *et al.*, 2012; Pedneault *et al.*, 2014; Tolar,
81 Ross, *et al.*, 2016). Despite the abundance of thaumarchaeal transcripts in
82 natural assemblages, we still have a poor understanding of how the relative
83 abundance of thaumarchaeal transcript markers such as *amoA*, *nirK* and
84 *ureC* relate to nutrient and energy availability across environmental
85 gradients.
86
87 Thaumarchaeal ammonia oxidation is initiated by the oxidation of ammonia
88 to hydroxylamine (NH_2OH) by the ammonia monooxygenase enzyme
89 complex (Amo) (Vajrala *et al.*, 2013), but the enzyme(s) catalyzing the
90 oxidation of NH_2OH to nitrite (NO_2^-) have not been confirmed (Walker *et al.*,
91 2010). Orthologs of the bacterial hydroxylamine oxidoreductase (Hao) or c-
92 type cytochrome synthesis and assembly machinery, thought to be required
93 for NH_2OH oxidation and electron transfer in ammonia-oxidizing bacteria
94 (AOB) (Arp *et al.*, 2007), are absent from all sequenced thaumarchaeal
95 genomes (Stahl and la Torre, 2012; Spang *et al.*, 2012; Kerou *et al.*, 2016).
96 Instead, unidentified Cu-containing metalloenzymes or F_{420}-dependent
97 monooxygenases are speculated to be involved in NH_2OH oxidation and
98 electron transfer to archaeal terminal oxidases (Walker *et al.*, 2010; Kerou
99 *et al.*, 2016) and may involve nitric oxide (NO) as either a direct
100 intermediate or an electron shuttle (Stieglmeier *et al.*, 2014; Martens-
101 Habbena *et al.*, 2015; Kozlowski *et al.*, 2016). While the precursor to NO
102 has not yet been elucidated, all free-living thaumarchaea with complete
103 genomes encode a Cu-containing multicopper oxidase with homology to
104 Cu-dependent nitrite reductases (NirK) that may be responsible for the
105 reduction of NO_2^- to NO (Kerou *et al.*, 2016).
106
107 '*Candidatus* Nitrosopelagicus brevis' str. CN25 is a cultured representative
108 of ubiquitous and abundant pelagic thaumarchaeal populations in the
109 shallow oligotrophic ocean (Santoro and Casciotti, 2011; Santoro *et al.*,
110 2015). Here, we describe the genome and transcriptome during urea-based
111 growth of a *Ca*. N. brevis strain that can utilize ammonia cleaved from urea
112 as a sole chemolithoautotrophic growth substrate. Additionally, we use *Ca*.
113 N. brevis str. CN25 to investigate the transcriptional response to ammonia
114 limitation in laboratory culture. These transcriptomes are further analyzed in

the context of several marine metatranscriptomes and used to identify conserved gene co-expression networks.

Results and Discussion

'*Candidatus* Nitrosopelagicus brevis' strain U25 genome and transcriptome: A urea-utilizing thaumarchaeon was obtained from an ammonia-oxidizing enrichment culture (Santoro and Casciotti, 2011) via subculturing with urea as a sole nitrogen and energy source (see 'Experimental Procedures') and used for the shotgun metagenome sequencing and experiments described here. After assembly and contig binning based on nucleotide frequencies and coverage, we obtained a three contig genome of this urea-utilizing thaumarchaeon (Supplementary Figure 1a). This genome is nearly identical to the *Ca*. N. brevis CN25 genome with regards to *i)* gene content; *ii)* genome organization (Supplementary Figure 1b); and *iii)* genome wide average nucleotide identity (99.99%; Supplementary Figure 2). We found 19 additional genes at four distinct genomic loci in this strain, relative to CN25 (Supplementary Table 1). The largest of these insertions (15 contiguous genes) includes 11 genes coding urea utilization machinery, including *ureABCDEFG*, which codes for urease and its chaperones, two urea sodium:solute symporter family (SSSF) transporters, a transcriptional regulator and several hypothetical proteins (Fig. 1a). We designate this urea-utilizing thaumarchaeon '*Candidatus* Nitrosopelagicus brevis' strain U25.

We sequenced a transcriptome from *Ca*. N. brevis str. U25 growing exponentially with urea as the growth substrate. Only one transcript from the chromosomal insertion containing the urea transport and metabolism genes (Fig. 1a) was among the top 50 transcripts detected: A7X95_00990, coding for a putative urea SSSF transporter (ranked 13.7 ± 0.33; mean ± SE, $n = 3$). Surprisingly, transcripts coding for catalytic urease components, or the second putative urea SSSF transporter (A7X95_00985) located immediately adjacent to A7X95_00990, were not nearly as abundant as A7X95_00990. For example, the mean expression levels of *ureC*, coding for the fused catalytic αβ-subunit of urease, and *ureA* (γ urease subunit) were 139 and 784-fold less abundant than that of A7X95_00990, respectively (ranked 390 ± 19.7 and 950 ± 50.8, respectively; mean ± SD, n=3). A7X95_00985, coding for the second urea SSSF transporter, was also expressed at a low level, comparable to *ureA*, ranked 940 ± 92.0.

153 During growth on urea, transcripts for genes coding for an ammonium
154 transporter (AMT1), ammonia monooxygenase subunits (*amoAB*) and
155 nitrite reductase (*nirK*) were within the top ten most abundant transcripts
156 detected in strain U25.
157
158 Although urea utilization genes have been detected in wild thaumarchaeal
159 populations, we have a poor understanding of how the abundances of
160 urease transcripts relate to growth and activity. To contextualize the
161 expression patterns observed in U25, we compared the relative rank of the
162 transcript abundances for only those genes coding for urea uptake and
163 catabolism (Fig. 1a) under laboratory growth conditions to the relative rank
164 of the transcript abundances of the same genes from several deeply
165 sequenced marine metatranscriptomes. The SSSF urea transporter
166 (A7X95_00990) was the most abundant urea-related gene transcript in
167 38% of the environmental datasets ($n = 8$) we investigated (Fig. 1b). In
168 contrast to culture conditions, where the SSSF urea transporter was the
169 most abundant urea-related gene transcript, *ureC* was the most abundant
170 transcript in 25% of the environmental datasets (Fig. 1b). This shows that
171 variability in the relative transcriptional activity of urea transport and
172 catabolism genes is not unusual. Our finding that *ureC* was not highly
173 expressed in exponentially growing cells also helps to explain previous field
174 observations of low *ureC* expression, and suggests the abundance of *ureC*
175 transcripts may be a poor molecular biomarker of active urea-based
176 nitrification. For example, *ureC* expression and urea-based nitrification
177 were found to be only weakly correlated across several environments
178 (Tolar, Wallsgrove, *et al.*, 2016), in contrast to high correlation between
179 *amoA* expression and ammonia oxidation rates (J. M. Smith *et al.*, 2014).
180 Similarly, in Arctic samples collected across seasons, *ureC* genes were
181 detected, yet *ureC* transcripts were only sporadically detected and at low
182 abundances (Pedneault *et al.*, 2014).
183
184 **Transcriptional response to ammonia limitation in '*Ca*. N. brevis'**
185 **strain CN25*:*** To understand adaptive mechanisms during ammonia
186 starvation, we explored the transcriptional response of *Ca*. N. brevis CN25
187 to ammonia limitation. A total of 51 gene transcripts were differentially
188 abundant when comparing the exponential growth phase of CN25 to
189 ammonia-limited stationary phase (generalized linear model likelihood ratio
190 test FDR ≤ 0.01 and ≥ 2-fold change in abundance; Supplementary Table

191 2). The gene transcripts that were significantly less abundant in stationary
192 phase included *amoA*, *amoB*, *nirK*, both *amtB*-like ammonium transporters
193 (AMT1=T478_1378; AMT2=T478_1350), several additional Cu-containing
194 metalloenzymes, and two ferredoxin-like 4Fe-4S binding domain proteins
195 (Fd1=T478_1472 and Fd2=T478_1259) (Fig. 2, Supplementary Table 2).
196 The downregulation of *amoA*, *amoB* and *nirK* in ammonia-limiting
197 conditions was recently shown for the ammonia-oxidizing thaumarchaeon
198 *Nitrosopumilus maritimus* using DNA microarrays (Qin *et al.*, 2017),
199 suggesting that one adaptation of ammonia-oxidizing archaea to ammonia
200 limitation is to reduce the relative expression of energy generation
201 machinery.
202
203 Only two genes, T478_1481, coding an Hsp20/α-crystallin domain small
204 heat shock protein, and T478_1394, annotated as a hypothetical protein,
205 were significantly more abundant (~10-fold) in ammonia-limited stationary
206 phase (Fig. 2, Supplementary Table 2). Hsp20 is a molecular chaperone
207 that enhances thermotolerance and binds to unfolded proteins to prevent
208 aggregation (Li *et al.*, 2011). The higher proportion of Hsp20 transcripts
209 and concomitant decrease in proportion of transcripts coding enzymes
210 integral to energy production suggests that one adaptation *Ca.* N. brevis
211 employs in ammonia-limited stationary phase may be to protect existing
212 proteins from degradation. Nutrient stress has been shown to induce the
213 expression of molecular chaperone proteins in ammonia-oxidizing archaea,
214 ammonia-oxidizing bacteria, and oligotrophic marine heterotrophs. For
215 example, in *N. maritimus*, two copies of Hsp20 were differentially
216 expressed during copper stress and recovery, but not during ammonia
217 starvation (Qin *et al.*, 2017). Similar to our findings regarding Hsp20,
218 *Nitrosomonas europaea* expressed peptides for the molecular chaperone
219 GroEL in both energy starved and energy replete conditions, but at
220 significantly greater levels under energy starvation (Pellitteri-Hahn *et al.*,
221 2011). The authors speculated that energy stress may induce chaperone
222 expression as part of a generalized stress response, and that these
223 chaperones are involved in protein protection (Pellitteri-Hahn *et al.*, 2011).
224 Similarly, the marine chemoorganoheterotroph '*Candidatus* Pelagibacter
225 ubique' induced GroEL protein expression under N-starvation (D. P. Smith
226 *et al.*, 2013), GroES under iron starvation (D. P. Smith *et al.*, 2010), and the
227 heat shock protein IpbA in nutrient-limited stationary phase (D. P. Smith *et*
228 *al.*, 2016). These finding suggest that one role of molecular chaperones

during nutrient stress may be to protect key enzymes from proteolytic turnover when cells scavenge peptides to support nutrient-limited sustenance.

In contrast to the finding that only two genes were more abundant in ammonia-limited stationary phase for *Ca*. N. brevis, over 200 genes were upregulated in ammonia-limited stationary phase for *N. maritimus* (Qin *et al*., 2017). One explanation for this observation is that *Ca*. N. brevis has a reduced capacity to sense and respond to environmental change as a result of its small genome (Santoro *et al*., 2015). Alternatively, our conservative statistical thresholding may have resulted in a reduced number of genes defined as differentially expressed. While it is important to note that our experimental design cannot distinguish between responses to energy limitation versus anabolic nitrogen limitation, transcriptional responses to ammonium limitation that involved the upregulation of only a few genes has been described for both ammonia-oxidizing bacteria and oligotrophic marine bacteria. For example, in the bacterium *N. europaea*, only 0.42% of the genome was upregulated under N-starvation (Wei *et al*., 2006). Similarly, '*Ca.* P. ubique,' exhibited a weak transcriptional response to N-starvation (D. P. Smith *et al*., 2013). The similar lack of transcriptional responses to nitrogen starvation by *Ca*. N. brevis and *Ca*. P. ubique are consistent with observations that organisms with small and potentially streamlined genomes have a limited capacity to respond rapidly to environmental change (Giovannoni *et al*., 2014; Cottrell and Kirchman, 2016; Giovannoni, 2017; Satinsky *et al*., 2017).

Despite significantly different transcript abundances of essential ammonia oxidation and transport genes across growth conditions, the rank order of these transcripts within a given treatment were similar, irrespective of growth condition. In particular, the most abundant gene transcripts in exponential phase were generally still the most abundant transcripts in ammonium-limited stationary phase (Fig. 2b). For example, transcripts for 32 genes (64%) were in the top 50 most abundant transcripts in both exponential and stationary phase (Fig. 2b). Interestingly, the abundances of 18 of these transcripts were also significantly different across treatments (Fig. 2b), illustrating that although transcripts can be differentially abundant across paired treatments, the changes in their relative cellular abundance may be subtler. Several of these consistently abundant but differentially

expressed transcripts are common molecular markers predicted to be essential for ammonia oxidation and transport, including the ammonium transporters AMT1 and AMT2, ammonia monooxygenase subunits (*amoAB*) and nitrite reductase (*nirK*). This suggests that the proportional changes we observed in highly-expressed genes may be the result of abundance changes in other genes that make up a smaller proportion of the transcriptome, such as Hsp20, and that even though we observe significant differences across treatments, the underlying transcript abundances might be similar.

The ammonia monooxygenase C subunit (AmoC) has been implicated in stress response (Berube and Stahl, 2012) and recovery from ammonia starvation in *N. europaea* (Berube *et al.*, 2007). The participation of AmoC in ammonium starvation appears to be conserved in thaumarchaeal ammonia oxidizers, where *amoC* transcript levels remained high in ammonia-limited stationary phase (Qin *et al.*, 2017). Consistent with these findings, *amoC* was abundant in both exponential and N-limited stationary phase in CN25 (the 13th and 7th most abundant transcript, respectively), and we did not observe a significant difference in the abundance of *amoC* across growth phases (Fig. 2).

Correlated gene expression across disparate environments: Controlled laboratory experiments such as those described above help us to understand gene regulation by isolating one experimental variable at a time. However, gene expression patterns observed in natural thaumarchaeal populations are the result of cells responding to complex and dynamic environmental conditions that can be cryptic and difficult to mimic in the laboratory. To identify clusters of co-expressed genes across disparate environmental conditions, and relate them to our laboratory findings, we constructed and analyzed a gene expression correlation network constructed from transcriptomes of exponentially growing CN25 and U25 cultures and marine metatranscriptomes. Although 64 metatranscriptomes were mapped to the *Ca*. N. brevis genomes, only ten met our strict criteria for inclusion in the network analysis presented here (see 'Experimental Procedures', below). The transcription of 1,407 of the 1,464 non-redundant genes in the two *Ca*. N. brevis genomes was significantly positively correlated with at least one other gene (Pearson's $r \geq 0.80$, $q \leq 0.025$; Fig. 3, Supplementary Table 3). Network modularity is a

305 measure of the group connectivity within a network, where connections
306 contained within a module are denser than connections between modules.
307 Modularity values range from -0.5 to 1, where 1 describes a highly modular
308 system. The modularity of this positive correlation network was 0.71,
309 indicating a high degree of modularity. Genes with positively correlated
310 expression organized into 38 groups (modules), ranging in membership
311 size from 2 to 236 genes (mean module size = 38.0 genes).
312
313 Genes encoding putative components of the core ammonia oxidation and
314 transport machinery are significantly co-expressed across distinct
315 environmental and laboratory conditions. A single 15-gene module (module
316 11 in Fig. 3) contained: *amoABCX*, AMT1, *nirK*, two PEFG-CTERM domain
317 proteins, Fd1 and Fd2, an Fe-S cluster assembly protein, a membrane
318 bound cupredoxin-containing protein, and three hypothetical proteins.
319 Further investigation of these hypothetical proteins suggests that
320 (T478_0057) is a putative archaeal cell division protein related to the
321 endosomal sorting complexes involved in membrane trafficking (ESCRT)-III
322 (Lindås *et al.*, 2008; Spang *et al.*, 2015). Our finding that *amoA*, *amoB* and
323 *nirK* transcripts are abundant and co-expressed with other genes coding for
324 membrane-bound Cu-containing metalloproteins (T478_1362 and
325 T478_0895) implies the products of these genes may participate in
326 ammonia oxidation. Previous speculation implicated membrane-bound
327 multicopper oxidases (Walker *et al.*, 2010; Stahl and la Torre, 2012;
328 Kozlowski *et al.*, 2016) or novel F_{420}-dependent monooxygenases (Kerou *et*
329 *al.*, 2016) in ammonia oxidation chemolithotrophy (specifically NH_2OH
330 oxidation) based on Cu redox chemistry or ortholog conservation across
331 thaumarchaeal genomes. However, the genes put forth in those studies
332 were not present in module 11 (referred to as the AMO module, herein),
333 suggesting they may not be involved in core energy metabolism (Fig. 3,
334 Supplementary Table 3). For example, a multicopper oxidase present in the
335 genomes of both *N. brevis* (T478_0261) and *N. maritimus* (Nmar_1663)
336 previously implicated to be involved in the oxidation of hydroxylamine to
337 nitrite (Walker *et al.*, 2010; Qin *et al.*, 2017) was not present in the AMO
338 module (Supplementary Table 3).
339
340 On average, the AMO module is expressed at a higher level than other
341 modules, and was more abundant in conditions where ammonia oxidation
342 rates and thaumarchaeal abundances would be predicted to be high (Fig.

343 4). For example, consistent with previous reports of higher ammonia
344 oxidation rates within hydrothermal plumes (Lam *et al.*, 2004), we show
345 that the AMO module is expressed highly within the Guyamas Deep
346 hydrothermal plume, relative to background samples (Fig. 4). Moreover,
347 similar to reports of increased thaumarchaeal gene expression in the
348 mesopelagic (Church *et al.*, 2010), the AMO module is less abundant in the
349 surface waters of Landsort Deep (0 and 5 m), relative to deeper waters (90
350 and 200 m) (Fig. 4).
351
352 **A new proposed model for thaumarchaeal chemolithotrophy via**
353 **ammonia oxidation:** A previous model of thaumarchaeal ammonia
354 oxidation proposed NO is derived from the reduction of NO_2^- by NirK, and
355 that this NO is subsequently used to oxidize NH_2OH (Kozlowski *et al.*,
356 2016). However, this model does not agree with tracer experiments using
357 ^{18}O labeled water, which show that only one O atom from water is
358 incorporated into NO_2^- produced by thaumarchaea (Santoro *et al.*, 2011;
359 Buchwald *et al.*, 2012). If NO_2^- was reduced to NO and used to produce
360 additional NO_2^-, the resulting NO_2^- would retain an average of more than
361 one O atom from water. Based on the co-expression data presented here,
362 we propose two alternative models of thaumarchaeal ammonia oxidation
363 that are consistent with previous isotope tracer data regarding the source of
364 O atoms in NO_2^-. In both models, NirK and two membrane-anchored
365 cupredoxins (T478_1362 and T478_0895) act in concert to oxidize NH_2OH
366 to NO_2^- in two steps: a three-electron oxidation of NH_2OH to NO, followed
367 by a one-electron oxidation of NO to NO_2^- (Supplementary Figure 3). The
368 involvement of T478_0895 orthologs in electron transfer with NirK, is
369 consistent with previous predictions based on gene expression data for *N.*
370 *maritimus* (Qin *et al.*, 2017). Both proposed pathways are also consistent
371 with the observed co-expression and high abundance of these transcripts
372 across distinct environmental conditions (Figs 2-4; (Hollibaugh *et al.*, 2011;
373 Baker *et al.*, 2012; Stewart *et al.*, 2012; Gifford *et al.*, 2013)). The predicted
374 localization of ammonia oxidation in the pseudoperiplasm (Walker *et al.*,
375 2010) is also a key aspect of the proposed models, as protein domain
376 analysis with InterPro (Jones *et al.*, 2014) indicates all proteins in these
377 models, and pertinent cupredoxin domains, are likely localized in the
378 pseudoperiplasmic space. While we cannot determine which reaction is
379 conducted by which Cu metalloenzyme, both scenarios are more

380 parsimonious than existing models and are plausible based on existing
381 bioinorganic chemistry literature.
382
383 Similar to the *N. maritimus* transcriptome and environmental
384 metatranscriptomes (Hollibaugh *et al.*, 2011; Williams *et al.*, 2012; Qin *et*
385 *al.*, 2017), ferredoxins were among the most highly expressed genes in *N.*
386 *brevis* (Fig. 2). However, we were surprised to find these ferredoxins (Fd1
387 and Fd2) and an Fe-S cluster assembly protein co-expressed with
388 ammonia oxidation genes in the AMO module. The co-expression of
389 ferredoxins in the AMO module suggests a central role for Fe-S cluster-
390 containing proteins in the electron transport chain of thaumarchaea. Both
391 Fd1 and Fd2 lack discernable signal sequences or PEFG domains,
392 suggesting that they are localized in the cytoplasm. Ferredoxin-containing
393 DNA binding transcriptional regulators have been implicated as NO sensors
394 (Kiley and Beinert, 2003). However, there are no predicted DNA-binding
395 domains in Fd1 or Fd2. Sequence structure threading of Fd1 and Fd2 with
396 phyre2 (Kelley *et al.*, 2015) returned best structural matches to NADH
397 dehydrogenase (ubiquinone) iron-sulfur protein 8 (threading confidence
398 score = 99.8% for both Fd1 and Fd2; coverage of Fd1 was 99% and 71%
399 for Fd2). Thus, we speculate that Fd1 and Fd2 participate in supplying
400 electrons to the ubiquinone pool, and thus may be involved in supplying the
401 electrons necessary to initiate ammonia oxidation via Amo.
402
403 Microbial gene expression is inherently modular. For example, functionally
404 related genes are often co-expressed in operons or regulons as a response
405 to external environmental signals (Freyre-Gonzales *et al.*, 2010). However,
406 the organization and patterns of population-level gene expression in
407 dynamic environments are poorly understood. Although we show a high
408 degree of modularity and correlated expression of a set of genes likely
409 involved in ammonia oxidation, the gene membership of the remaining
410 modules did not reveal a clear pattern of how the genes contained within a
411 given module are functionally related (Supplementary Table 3). For
412 example, genes coding for the modified 3-hydroxypropioinate/ 4-
413 hydroxybutryrate carbon fixation pathway proteins are dispersed across
414 five modules (module numbers 3, 4, 18, 21, and 36; Fig. 3 and
415 Supplementary Table 3). Similarly, vitamin B_{12}-production genes are spread
416 across eight modules (module numbers 1, 3, 4, 10, 12, 18, 21, and 26; Fig.
417 3 and Supplementary Table 3). The structure of the transcription co-

418 expression network illustrated in Fig. 3 is consistent with the interpretation
419 that thaumarchaeal population-level regulatory organization is structured in
420 a decentralized manner. One explanation for this organization may be that
421 decentralized expression networks may help to buffer gene expression
422 changes or maintain genetic diversity in dynamic environments through a
423 suite of feedbacks without centralized regulatory mechanisms (Hartwell *et*
424 *al*., 1999).
425
426 Other reasons the gene membership in the co-expression modules may not
427 reveal clear functional relationships may stem from the environments
428 sampled or the analysis techniques used. For example, our methods likely
429 underestimate the true modularity of *Ca*. N. brevis gene expression. Some
430 of the larger expression modules may comprise distinct modules that we
431 could not resolve because we did not sample an environment with
432 physicochemical parameters necessary to resolve subtle gene expression
433 patterns. Second, although our goal was to be conservative in our network
434 construction, we may be missing important network structural components
435 because of the thresholding parameters or our analysis techniques. Further
436 resolution of such gene expression patterns would require deeply
437 sequenced metatranscriptomes from additional distinct environments and
438 transcriptome analysis of additional thaumarchaea grown under diverse
439 culture conditions. Future research into understanding why certain genes or
440 pathways are co-expressed with one another, and how transcript
441 abundances manifest into functional potential in each environment or
442 culture setting would be necessary to fully disentangle the gene expression
443 we observe here.
444
445 **Conclusions:**
446 Here we show the rank of most thaumarchaeal transcripts reported as
447 being abundant in the environment (*amoABC*, both *amtB* genes and *nirK*,
448 for example) are relatively invariant across growth phases and
449 environmental conditions. That is, within a given treatment, abundant
450 genes are consistently proportionally abundant, irrespective of growth
451 condition. However, consistent with other studies of thaumarchaeal
452 transcription, the proportions of some of these genes were indeed
453 significantly differentially abundant across paired treatments, indicating
454 ammonia availability did affect the proportional abundances of ammonia
455 oxidation and transport transcripts. One explanation for this observation is

456 that although these transcripts are not 'constitutive' in a classic sense (that
457 is, they are differentially abundant across paired experiments), they are
458 instead 'affluent,' in that they make up a large part of the total transcript
459 pool, irrespective of growth condition.
460
461 Discovering gene function in fastidious or uncultivated lineages remains
462 one of the biggest challenges in environmental microbiology. Narrowing the
463 scope of targets for detailed biochemical investigation is difficult because
464 manipulative experiments are limited in their ability to identify networks of
465 co-regulated genes by the number of environmental parameters we can
466 recreate in a laboratory. The approach used here leverages *in situ*
467 transcript abundance data - in which the environmental conditions are
468 incompletely characterized - to identify genes that share similar
469 transcription patterns. In addition to our putative models of ammonia
470 oxidation in thaumarchaea, this approach shows that 4Fe-4S cluster-
471 containing proteins likely have an important role in ammonia oxidation,
472 indicating a role for iron in archaeal nitrification, which has been previously
473 under appreciated. Detailed biochemical characterization of NirK, other
474 cupredoxin-containing proteins, Fd1 and Fd2 is the next step in
475 understanding their specific role in core thaumarchaeal energy metabolism.
476
477 **Methods:**
478 *Organism sources:* Both '*Candidatus* Nitrosopelagicus brevis' str. CN25
479 and '*Ca.* N. brevis' str. U25 were obtained from an ammonia-oxidizing
480 enrichment culture previously known as CN25 (Santoro and Casciotti,
481 2011) grown on Oligotrophic North Pacific Medium. Oligotrophic North
482 Pacific Medium (ONP) consists of natural seawater, a
483 chemolithoautotrophic nitrogen source (NH_4Cl or urea), ampicillin (10.8
484 µM), streptomycin (68.6 µM), potassium phosphate (29.4 µM), and a
485 chelated trace metal mix consisting of disodium ethylenediaminetetraacetic
486 acid (14 µM), $FeCl_2$ (7.25 µM), $ZnCl_2$ (0.5 µM), $MnCl_2$ (0.5 µM), H_3BO_3 (1
487 µM), $CoCl_2$-$6H_2O$ (0.8 µM), $CuCl_2$-$2H_2O$ (0.1 µM), $NiCl_2$-H_2O (0.1 µM),
488 Na_2MoO_4-$2H_2O$ (0.15 µM). Preliminary metagenomic sequencing of the
489 original CN25 enrichment indicated the presence of urease genes in a
490 minority of the archaeal population. Sequential transfers of the initial
491 enrichment were made into ONP (Santoro and Casciotti, 2011) amended
492 with 50-100 µM urea, instead of NH_4Cl, over a period of ~48 months. In
493 parallel, separate transfers of the CN25 enrichment culture were

494 propagated using NH_4Cl as a nitrogen and energy source, but without the
495 use of streptomycin, which could potentially serve as a source of urea
496 (Klein and Pramer, 1961). The enrichment culture resulting from the
497 propagation with NH_4Cl did not contain amplifiable *ureC* genes by PCR,
498 using the archaeal-specific ureC primers Thaum_UreC F and Thaum_UreC
499 R (Yakimov *et al.*, 2011) before the sequencing and genome analysis
500 described elsewhere (Santoro *et al.*, 2015).
501
502 *General cultivation conditions:* All thaumarchaeal enrichments were
503 propagated in in ONP medium in a base of aged natural seawater
504 (collected from 10 m depth at 15°S, 173°W on 23 October 2011; 0.2 µm
505 pore size filtered at sea) amended with 50 or 100 µM NH_4Cl or 100 µM
506 urea as the chemolithoautotrophic substrate. All cultures were propagated
507 in 250 mL polycarbonate flasks at 22°C in the dark and monitored for NO_2^-
508 production using the Griess reagent colorimetric method (Strickland and
509 Parsons, 1972). Cell counts were obtained with a Millipore Guava
510 EasyCyte 5HT flow cytometer as described previously (Tripp, 2008).
511
512 *Cell harvesting for and genome sequencing of 'Ca. N. brevis' str. U25:* The
513 *Ca*. N. brevis U25 enrichment culture that was grown exclusively with urea
514 as the sole chemolithoautotrophic growth substrate for >50 generations,
515 was harvested by filtration on to 25 mm diameter, 0.22 µm pore-size Supor-
516 200 filters and frozen at -80°C. DNA was extracted using a DNeasy blood &
517 Tissue DNA extraction kit (Qiagen, Valencia, CA, USA), following the
518 manufacturer's instructions. The DNA was treated with RNAse and
519 examined using a Bioanlayzer 2100 (Agilent) with 500 ng serving as the
520 input for library construction (NEBNext paired-end DNA Library Prep kit,
521 New England Biolabs). The sample was sequenced on an Illumina MiSEQ
522 (v2 chemistry, paired 250 bp reads). Reads were quality trimmed and
523 served as the inputs to assembly with metaSPAdes (v 0.5, 70mer) (Nurk *et*
524 *al.*, 2017). The K-mer usage and phylogenetic annotation of the assembled
525 contigs were then used to visually identify a putative thaumarchaeal bin
526 (Supplementary Figure 1a) (Laczny *et al.*, 2015). The 3 contig genome was
527 annotated using the JGI IMG pipeline (img.jgi.doe.gov) and the PGAP
528 pipeline at NCBI (Zhao *et al.*, 2011).
529
530 *Experimental design, cell harvesting and RNA extraction for culture*
531 *transcriptomes:* For experiments investigating the effects of ammonia

532 limitation, ONP medium was amended with 50 µM NH_4Cl as the
533 chemolithoautotrophic growth substrate. In this experiment, six replicates
534 were prepared, three of which were harvested in late exponential phase
535 (Exponential phase) and three of which were harvested in late NH_4Cl-
536 limited stationary phase (Stationary phase) (Supplementary Fig. 4). We
537 deliberately harvested the exponential phase cultures in late exponential
538 phase to ensure maximal cell biomass for transcriptome analysis. The
539 length of starvation in stationary-phase was based on the exponential-
540 phase doubling time of seven days, approximately the population doubling
541 time during exponential growth. NH_4Cl-limitation in this phase is supported
542 by a linear dose response in maximal cell density to NH_4Cl additions
543 (Supplementary Fig. 5).
544
545 Transcriptomes that were included in the network analysis were obtained
546 from distinct, mid-exponential phase *Ca*. N. brevis strains CN25 and U25,
547 that were growing on ONP medium amended with either 100 µM NH_4Cl
548 (str. CN25; n=3) or 100 µM urea (str. U25; n=3) as growth substrates,
549 respectively (Supplementary Fig. 6). Cells were harvested by filtration on to
550 25 mm diameter, 0.22 µm pore-size Supor-200 filters and frozen at -80°C.
551 For RNA extraction, cells were disrupted as described in (Santoro *et al.*,
552 2010). RNA was extracted using TRIzol LS reagent (Ambion-Life
553 Technologies) per the manufacturer's instructions and stored in nuclease-
554 free water at -80°C. Urea consumption by str. U25 was determined
555 colorimetrically using the diacetyl monoxime method (Price and Harrison,
556 1987) (Supplementary Fig. 7).
557
558 *Transcriptome sequencing and mapping for culture experiments:*
559 Transcriptome samples were prepared for sequencing using the TotalScript
560 RNA-Seq kit (Epicentre-Illumina), which biases against rRNA, using the
561 manufacturer recommended protocol. Libraries were trial sequenced on an
562 Illumina MiSEQ to determine uniformity between barcodes and then fully
563 sequenced in one 300 cycle NextSEQ run which generated 246.6 million
564 paired-end 150 bp reads. Raw Illumina reads in fastq format were
565 interleaved to match paired ends. Sequencing primers and barcode
566 indexes were identified by BLAST against the NCBI vector database and
567 trimmed along with regions with Q scores < 30. Reads mapping to
568 ribosomal RNAs were identified and removed using ribopicker (Schmieder
569 *et al.*, 2011). Reads were then mapped to *Ca*. N. brevis genomes at 90%

570 nucleotide identity with CLC Genomics Workbench (command:
571 clc_ref_assemble –s 0.9). Raw read counts per open reading frame (ORF)
572 were compiled.
573
574 *Analysis of differentially abundant gene transcripts:* Differential gene
575 abundance analysis was performed using a generalized linear model
576 likelihood ratio test in the edgeR software package (v 3.8.5) (Robinson and
577 Smyth, 2008). We defined significant differential abundance as those
578 genes with a false discovery rate (FDR) ≤ 0.01 and greater than 2-fold
579 abundance change across treatments.
580
581 *Rank Analyses:* Raw read counts per ORF were scaled to expression units
582 of reads per base per million reads mapped (RPKM=(10^6 * C)/(NL/10^3))
583 where C is the number of transcript reads mapped to an ORF; N is total
584 reads mapped to all ORFs in the genome; and L is the ORF length in base
585 pairs (Mortazavi *et al.*, 2008). RPKM values were subsequently ranked,
586 with a rank of 1 depicting the most abundant transcript within a given
587 treatment. Rank ties within a treatment were averaged.
588
589 *Metatranscriptome mapping to genomes of Ca. N. brevis strains:* Sequence
590 reads from 68 metatranscriptomes were mapped to the *Ca*. N. brevis
591 genomes at 50% nucleotide identity using CLC Genomics Workbench
592 (command: clc_ref_assemble –s 0.5) (Supplementary Table 4). The
593 number of metatranscriptome reads that mapped to the *Ca*. N. brevis
594 genomes were variable and ranged from 10 reads to 236,954 reads and
595 mapped to 0.5-89% of the unique genes in the *Ca*. N. brevis genomes
596 (Supplementary Table 4). Raw read counts per ORF were then compiled
597 (ORF n=1445 for str. CN25 and n=1461 for U25).
598
599 *Network construction:* Only those metatranscriptomes that mapped to
600 ≥45% of the ORFs in the *Ca*. N. brevis genomes, along with the
601 transcriptomes from *Ca*. N. brevis strains CN25 and U25 growing in
602 exponential phase initiated with 100 µM NH_4Cl or urea, respectively, were
603 included for network analysis. Of the 68 metatranscriptomes mapped to the
604 *Ca*. N. brevis genomes, only ten passed this filtering step and were used
605 for network analysis (Supplementary Table 4). Read counts were scaled to
606 RPKM expression units. RPKM scores calculated for individual culture
607 transcriptome replicates were averaged (n=3) to avoid pseudo-replication

effects in the network. The resulting RPKM expression values were rank-normalized to Van der Waerden (VdW) scores using the formula ($s = \Phi^{-1}(r / (n+1))$), where s is the VdW score for a gene, r is the rank for that observation, n is the sample size and Φ is the Φth quantile from the standard normal distribution using *tRank* in the multic R package (Lunde *et al.*). Pearson correlation coefficients and *P* value estimates were calculated for all gene:gene pairs across the VdW-normalized metatranscriptomes and culture experiments (n=10 and 2, respectively) with the *rcorr* command in the Hmisc R package (Harrell and Dupont). To correct for multiple hypothesis testing, *q* values were computed from *P* value estimates using the qvalue R package (Storey and Tibshirani, 2003). Correlations with a *q* value ≤ 0.025 were used for network analysis. All correlations at this threshold were strongly correlated (Pearson's $r \geq 0.8$).

Network Statistics: Network modularity and module membership were calculated in Gephi (0.8.2 beta) with the following settings: resolution 1.0, randomized and unweighted (Blondel *et al.*, 2008). The resulting network was visualized using the Fruchterman-Reingold algorithm in Gephi.

Data Availability/Sources:

Transcriptomes from *Ca*. N. brevis str. CN25 and U25 can be found in the NCBI BioSample archive under accession numbers SAMN6290440-6290457. The U25 genome has been deposited at DDBJ/ENA/GenBank under the accession LXWN00000000. The version described in this paper is version LXWN01000000. The metatranscriptomic data from Landsort Deep in the Baltic is available from the Sequence Read Archive under numbers SAMN04943349-SAMN04943415.
Other metatranscriptomes analyzed in the network are publically available through iMicrobe (https://imicrobe.us) or NCBI's Short Read Archive through the following accession numbers: CAM_PROJ_Sapelo2008, CAM_PROJ_AmazonRiverPlume, CAM_PROJ_PacificOcean, CAM_P_0000545, SRA023632.1.

Acknowledgements:

This research was supported by NSF awards OCE-1260006, OCE-1437310, and DBI-1318455 to AES. CLD was supported by NSF OCE-1259994. We thank Matt Rawls for urea measurements, Mike Stukel for

obtaining oligotrophic seawater, and Albert Barberán and Jason Corwin for discussions regarding network construction. AES is an Alfred P. Sloan Research Fellow in Ocean Sciences.

References:

Alonso-Sáez, L., Waller, A.S., Mende, D.R., Bakker, K., Farnelid, H., Yager, P.L., et al. (2012) Role for urea in nitrification by polar marine Archaea. *Proc. Natl. Acad. Sci. U.S.A.* **109**: 17989–17994.

Arp, D.J., Chain, P.S.G., and Klotz, M.G. (2007) The impact of genome analyses on our understanding of ammonia-oxidizing bacteria. *Annu. Rev. Microbiol.* **61**: 503–528.

Baker, B.J., Lesniewski, R.A., and Dick, G.J. (2012) Genome-enabled transcriptomics reveals archaeal populations that drive nitrification in a deep-sea hydrothermal plume. *The ISME Journal* **6**: 2269–2279.

Bayer, B., Vojvoda, J., Offre, P., Alves, R.J.E., Elisabeth, N.H., Garcia, J.A., et al. (2015) Physiological and genomic characterization of two novel marine thaumarchaeal strains indicates niche differentiation. *The ISME Journal* **10**: 1051–1063.

Beman, J.M., Popp, B.N., and Alford, S.E. (2012) Quantification of ammonia oxidation rates and ammonia-oxidizing archaea and bacteria at high resolution in the Gulf of California and eastern tropical North Pacific Ocean. *Limnol. Oceangr.* **57**: 711–726.

Berube, P.M. and Stahl, D.A. (2012) The divergent AmoC3 subunit of ammonia monooxygenase functions as part of a stress response system in *Nitrosomonas europaea*. *Journal of Bacteriology* **194**: 3448–3456.

Berube, P.M., Samudrala, R., and Stahl, D.A. (2007) Transcription of all amoC copies is associated with recovery of *Nitrosomonas europaea* from ammonia starvation. *Journal of Bacteriology* **189**: 3935–3944.

Blondel, V.D., Guillaume, J.-L., Lambiotte, R., and Lefebvre, E. (2008) Fast unfolding of communities in large networks. *Journal of Statistical Mechanics: Theory and Experiment* **10**: 10008–.

Buchwald, C., Santoro, A.E., McIlvin, M.R., and Casciotti, K.L. (2012) Oxygen isotopic composition of nitrate and nitrite produced by nitrifying cocultures and natural marine assemblages. *Limnol. Oceangr.* **57**: 1361–1375.

Church, M.J., Wai, B., Karl, D.M., and DeLong, E.F. (2010) Abundances of

684 crenarchaeal *amoA* genes and transcripts in the Pacific Ocean.
685 *Environmental Microbiology* **12**: 679–688.
686 Coolen, M.J.L., Abbas, B., van Bleijswijk, J., Hopmans, E.C., Kuypers,
687 M.M.M., Wakeham, S.G., and Sinninghe Damsté, J.S. (2007) Putative
688 ammonia-oxidizing Crenarchaeota in suboxic waters of the Black Sea: a
689 basin-wide ecological study using 16S ribosomal and functional genes
690 and membrane lipids. *Environmental Microbiology* **9**: 1001–1016.
691 Cottrell, M.T. and Kirchman, D.L. (2016) Transcriptional control in marine
692 copiotrophic and oligotrophic bacteria with streamlined genomes.
693 *Applied and Environmental Microbiology* **82**: 6010–6018.
694 Francis, C.A., Roberts, K.J., Beman, J.M., Santoro, A.E., and Oakley, B.B.
695 (2005) Ubiquity and diversity of ammonia-oxidizing archaea in water
696 columns and sediments of the ocean. *Proc. Natl. Acad. Sci. U.S.A.* **102**:
697 14683–14688.
698 Freyre-Gonzales, J.A., Educ, L.T.-Q.N., 2010 (2010) Analyzing regulatory
699 networks in bacteria. *Nature Education* **3**: 24–27.
700 Gifford, S.M., Sharma, S., Booth, M., and Moran, M.A. (2013) Expression
701 patterns reveal niche diversification in a marine microbial assemblage.
702 *The ISME Journal* **7**: 281–298.
703 Giovannoni, S.J. (2017) SAR11 Bacteria: The most abundant plankton in
704 the oceans. *Annu. Rev. Marine. Sci.* **9**: 231–255.
705 Giovannoni, S.J., Cameron Thrash, J., and Temperton, B. (2014)
706 Implications of streamlining theory for microbial ecology. *The ISME*
707 *Journal* **8**: 1553–1565.
708 Harrell, F.E., Jr and Dupont, C. Hmisc: Harrell Miscellaneous.
709 Hartwell, L.H., Hopfield, J.J., Leibler, S., and Murray, A.W. (1999) From
710 molecular to modular cell biology. *Nature* **402**: C47–C52.
711 Hollibaugh, J.T., Gifford, S., Sharma, S., Bano, N., and Moran, M.A. (2011)
712 Metatranscriptomic analysis of ammonia-oxidizing organisms in an
713 estuarine bacterioplankton assemblage. *The ISME Journal* **5**: 866–878.
714 Jones, P., Binns, D., Chang, H.-Y., Fraser, M., Li, W., McAnulla, C., et al.
715 (2014) InterProScan 5: genome-scale protein function classification.
716 *Bioinformatics* **30**: 1236–1240.
717 Karner, M.B., Delong, E.F., and Karl, D.M. (2001) Archaeal dominance in
718 the mesopelagic zone of the Pacific Ocean. *Nature* **409**: 507–510.
719 Kelley, L.A., Mezulis, S., Yates, C.M., Wass, M.N., and Sternberg, M.J.E.
720 (2015) The Phyre2 web portal for protein modeling, prediction and
721 analysis. *Nat Protoc* **10**: 845–858.

722 Kerou, M., Offre, P., Valledor, L., Abby, S.S., Melcher, M., Nagler, M., et al.
723 (2016) Proteomics and comparative genomics of *Nitrososphaera*
724 *viennensis* reveal the core genome and adaptations of archaeal
725 ammonia oxidizers. *Proc. Natl. Acad. Sci. U.S.A.* 201601212–19.
726 Kiley, P.J. and Beinert, H. (2003) The role of Fe–S proteins in sensing and
727 regulation in bacteria. *Current Opinion in Microbiology* **6**: 181–185.
728 Klein, D. and Pramer, D. (1961) Bacterial dissimilation of streptomycin.
729 *Journal of Bacteriology* **82**: 505–510.
730 Kozlowski, J.A., Stieglmeier, M., Schleper, C., Klotz, M.G., and Stein, L.Y.
731 (2016) Pathways and key intermediates required for obligate aerobic
732 ammonia-dependent chemolithotrophy in bacteria and
733 Thaumarchaeota. *The ISME Journal* **10**: 1836–1845.
734 Laczny, C.C., Sternal, T., Plugaru, V., Gawron, P., Atashpendar, A.,
735 Margossian, H., et al. (2015) VizBin - an application for reference-
736 independent visualization and human-augmented binning of
737 metagenomic data. *Microbiome* **3**: 1–7.
738 Lam, P., Cowen, J.P., and Jones, R.D. (2004) Autotrophic ammonia
739 oxidation in a deep-sea hydrothermal plume. *FEMS Microbiology*
740 *Ecology* **47**: 191–206.
741 Lam, P., Lavik, G., Jensen, M.M., van de Vossenberg, J., Schmid, M.,
742 Woebken, D., et al. (2009) Revising the nitrogen cycle in the Peruvian
743 oxygen minimum zone. *Proc. Natl. Acad. Sci. U.S.A.* **106**: 4752–4757.
744 Li, D.-C., Yang, F., Lu, B., Chen, D.-F., and Yang, W.-J. (2011)
745 Thermotolerance and molecular chaperone function of the small heat
746 shock protein HSP20 from hyperthermophilic archaeon, *Sulfolobus*
747 *solfataricus P2*. *Cell Stress and Chaperones* **17**: 103–108.
748 Lindås, A.-C., Karlsson, E.A., Lindgren, M.T., Ettema, T.J.G., and
749 Bernander, R. (2008) A unique cell division machinery in the Archaea.
750 *Proc. Natl. Acad. Sci. U.S.A.* **105**: 18942–18946.
751 Lunde, E., de Andrade, M., Atkinson, B., and Votruba, P. multic:
752 Quantitative linkage analysis tools using the variance
753 components approach.
754 Martens-Habbena, W., Qin, W., Horak, R.E.A., Urakawa, H., Schauer, A.J.,
755 Moffett, J.W., et al. (2015) The production of nitric oxide by marine
756 ammonia-oxidizing archaea and inhibition of archaeal ammonia
757 oxidation by a nitric oxide scavenger. *Environmental Microbiology* **17**:
758 2261–2274.
759 Mortazavi, A., Williams, B.A., McCue, K., Schaeffer, L., and Wold, B.

760 (2008) Mapping and quantifying mammalian transcriptomes by RNA-
761 Seq. *Nat Meth* **5**: 621–628.
762 Nakagawa, T. and Stahl, D.A. (2013) Transcriptional response of the
763 archaeal ammonia oxidizer *Nitrosopumilus maritimus* to low and
764 environmentally relevant ammonia concentrations. *Applied and*
765 *Environmental Microbiology* **79**: 6911–6916.
766 Nurk, S., Meleshko, D., Korobeynikov, A., and Pevzner, P.A. (2017)
767 metaSPAdes: a new versatile metagenomic assembler. *Genome*
768 *Research* **27**: 824–834.
769 Pedneault, E., Galand, P.E., Potvin, M., Tremblay, J.-É., and Lovejoy, C.
770 (2014) Archaeal *amoA* and *ureC* genes and their transcriptional activity
771 in the Arctic Ocean. *Sci. Rep.* **4**: 1–11.
772 Pellitteri-Hahn, M.C., Halligan, B.D., Scalf, M., Smith, L., and Hickey, W.J.
773 (2011) Quantitative proteomic analysis of the chemolithoautotrophic
774 bacterium *Nitrosomonas europaea*: Comparison of growing- and
775 energy-starved cells. *Journal of Proteomics* **74**: 411–419.
776 Pitcher, A., Villanueva, L., Hopmans, E.C., Schouten, S., Reichart, G.-J.,
777 and Sinninghe Damsté, J.S. (2011) Niche segregation of ammonia-
778 oxidizing archaea and anammox bacteria in the Arabian Sea oxygen
779 minimum zone. *The ISME Journal* **5**: 1896–1904.
780 Price, N.M. and Harrison, P.J. (1987) Comparison of methods for the
781 analysis of dissolved urea in seawater. *Marine Biology* **94**: 307–317.
782 Qin, W., Amin, S.A., Lundeen, R.A., Heal, K.R., Martens-Habbena, W.,
783 Turkarslan, S., et al. (2017) Stress response of a marine ammonia-
784 oxidizing archaeon informs physiological status of environmental
785 populations. *The ISME Journal* 1–12.
786 Qin, W., Amin, S.A., Martens-Habbena, W., Walker, C.B., Urakawa, H.,
787 Devol, A.H., et al. (2014) Marine ammonia-oxidizing archaeal isolates
788 display obligate mixotrophy and wide ecotypic variation. *Proc. Natl.*
789 *Acad. Sci. U.S.A.* **111**: 12504–12509.
790 Robinson, M.D. and Smyth, G.K. (2008) Small-sample estimation of
791 negative binomial dispersion, with applications to SAGE data.
792 *Biostatistics* **9**: 321–332.
793 Santoro, A.E. and Casciotti, K.L. (2011) Enrichment and characterization of
794 ammonia-oxidizing archaea from the open ocean: phylogeny,
795 physiology and stable isotope fractionation. *The ISME Journal* **5**: 1796–
796 1808.
797 Santoro, A.E., Buchwald, C., McIlvin, M.R., and Casciotti, K.L. (2011)

Isotopic signature of N_2O produced by marine ammonia-oxidizing archaea. *Science* **333**: 1282–1285.

Santoro, A.E., Casciotti, K.L., and Francis, C.A. (2010) Activity, abundance and diversity of nitrifying archaea and bacteria in the central California Current. *Environmental Microbiology* **12**: 1989–2006.

Santoro, A.E., Dupont, C.L., Richter, R.A., Craig, M.T., Carini, P., McIlvin, M.R., et al. (2015) Genomic and proteomic characterization of "*Candidatus* Nitrosopelagicus brevis": an ammonia-oxidizing archaeon from the open ocean. *Proc. Natl. Acad. Sci. U.S.A.* **112**: 1173–1178.

Satinsky, B.M., Smith, C.B., Sharma, S., Ward, N.D., Krusche, A.V., Richey, J.E., et al. (2017) Patterns of Bacterial and Archaeal gene expression through the lower Amazon River. *Front. Mar. Sci.* **4**: 1937–15.

Schattenhofer, M., Fuchs, B.M., Amann, R., Zubkov, M.V., Tarran, G.A., and Pernthaler, J. (2009) Latitudinal distribution of prokaryotic picoplankton populations in the Atlantic Ocean. *Environmental Microbiology* **11**: 2078–2093.

Schmieder, R., Lim, Y.W., and Edwards, R. (2011) Identification and removal of ribosomal RNA sequences from metatranscriptomes. *Bioinformatics* **28**: 433–435.

Shi, Y., Tyson, G.W., Eppley, J.M., and DeLong, E.F. (2010) Integrated metatranscriptomic and metagenomic analyses of stratified microbial assemblages in the open ocean. *The ISME Journal* **5**: 999–1013.

Smith, D.P., Kitner, J.B., Norbeck, A.D., Clauss, T.R., Lipton, M.S., Schwalbach, M.S., et al. (2010) Transcriptional and translational regulatory responses to iron limitation in the globally distributed marine bacterium *'Candidatus* Pelagibacter ubique'. *PLoS ONE* **5**: e10487–10.

Smith, D.P., Nicora, C.D., Carini, P., Lipton, M.S., Norbeck, A.D., Smith, R.D., and Giovannoni, S.J. (2016) Proteome remodeling in response to sulfur limitation in "*Candidatus* Pelagibacter ubique." *mSystems* **1**: e00068–16–15.

Smith, D.P., Thrash, J.C., Nicora, C.D., Lipton, M.S., Burnum-Johnson, K.E., Carini, P., et al. (2013) Proteomic and transcriptomic analyses of "*Candidatus* Pelagibacter ubique" describe the first PII-independent response to nitrogen limitation in a free-living Alphaproteobacterium. *mBio* **4**: e00133–12.

Smith, J.M., Casciotti, K.L., Chavez, F.P., and Francis, C.A. (2014) Differential contributions of archaeal ammonia oxidizer ecotypes to

836 nitrification in coastal surface waters. *The ISME Journal* **8**: 1704–1714.
837 Spang, A., Poehlein, A., Offre, P., Zumbrägel, S., Haider, S., Rychlik, N., et
838 al. (2012) The genome of the ammonia-oxidizing '*Candidatus*
839 Nitrososphaera gargensis': insights into metabolic versatility and
840 environmental adaptations. *Environmental Microbiology* **14**: 3122–3145.
841 Spang, A., Saw, J.H., Jørgensen, S.L., Zaremba-Niedzwiedzka, K., Martijn,
842 J., Lind, A.E., et al. (2015) Complex archaea that bridge the gap
843 between prokaryotes and eukaryotes. *Nature* **521**: 173–179.
844 Stahl, D.A. and la Torre, de, J.R. (2012) Physiology and diversity of
845 ammonia-oxidizing archaea. *Annu. Rev. Microbiol.* **66**: 83–101.
846 Stewart, F.J., Ulloa, O., and DeLong, E.F. (2012) Microbial
847 metatranscriptomics in a permanent marine oxygen minimum zone.
848 *Environmental Microbiology* **14**: 23–40.
849 Stieglmeier, M., Mooshammer, M., Kitzler, B., Wanek, W., Zechmeister-
850 Boltenstern, S., Richter, A., and Schleper, C. (2014) Aerobic nitrous
851 oxide production through N-nitrosating hybrid formation in ammonia-
852 oxidizing archaea. *The ISME Journal* **8**: 1135–1146.
853 Storey, J.D. and Tibshirani, R. (2003) Statistical significance for
854 genomewide studies. *Proc. Natl. Acad. Sci. U.S.A.* **100**: 9440–9445.
855 Strickland, J.D.H. and Parsons, T.R. (1972) A Practical Handbook of
856 Seawater Analysis. 2.ed.
857 Tolar, B.B., Ross, M.J., Wallsgrove, N.J., Liu, Q., Aluwihare, L.I., Popp,
858 B.N., and Hollibaugh, J.T. (2016) Contribution of ammonia oxidation to
859 chemoautotrophy in Antarctic coastal waters. *The ISME Journal* **10**:
860 2605–2619.
861 Tolar, B.B., Wallsgrove, N.J., Popp, B.N., and Hollibaugh, J.T. (2016)
862 Oxidation of urea-derived nitrogen by thaumarchaeota-dominated
863 marine nitrifying communities. *Environmental Microbiology*.
864 Tripp, H.J. (2008) Counting marine microbes with Guava Easy-Cyte 96 well
865 plate reading flow cytometer. *Protocol Exchange*.
866 Vajrala, N., Martens-Habbena, W., Sayavedra-Soto, L.A., Schauer, A.,
867 Bottomley, P.J., Stahl, D.A., and Arp, D.J. (2013) Hydroxylamine as an
868 intermediate in ammonia oxidation by globally abundant marine
869 archaea. *Proc. Natl. Acad. Sci. U.S.A.* **110**: 1006–1011.
870 Walker, C.B., la Torre, de, J.R., Klotz, M.G., Urakawa, H., Pinel, N., Arp,
871 D.J., et al. (2010) *Nitrosopumilus maritimus* genome reveals unique
872 mechanisms for nitrification and autotrophy in globally distributed
873 marine crenarchaea. *Proc. Natl. Acad. Sci. U.S.A.* **107**: 8818–8823.

874 Wei, X., Yan, T., Hommes, N.G., Liu, X., Wu, L., McAlvin, C., et al. (2006)
875 Transcript profiles of *Nitrosomonas europaea* during growth and upon
876 deprivation of ammonia and carbonate. *FEMS Microbiology Letters* **257**:
877 76–83.
878 Williams, T.J., Long, E., Evans, F., DeMaere, M.Z., Lauro, F.M., Raftery,
879 M.J., et al. (2012) A metaproteomic assessment of winter and summer
880 bacterioplankton from Antarctic Peninsula coastal surface waters. *The*
881 *ISME Journal* **6**: 1883–1900.
882 Yakimov, M.M., La Cono, V., Smedile, F., DeLuca, T.H., rez, S.J.A.,
883 Ciordia, S., et al. (2011) Contribution of crenarchaeal autotrophic
884 ammonia oxidizers to the dark primary production in Tyrrhenian deep
885 waters (Central Mediterranean Sea). *The ISME Journal* **5**: 945–961.
886 Zhao, Y., Wu, J., Yang, J., Sun, S., Xiao, J., and Yu, J. (2011) PGAP: pan-
887 genomes analysis pipeline. *Bioinformatics* **28**: 416–418.
888
889

890 **Figures:**

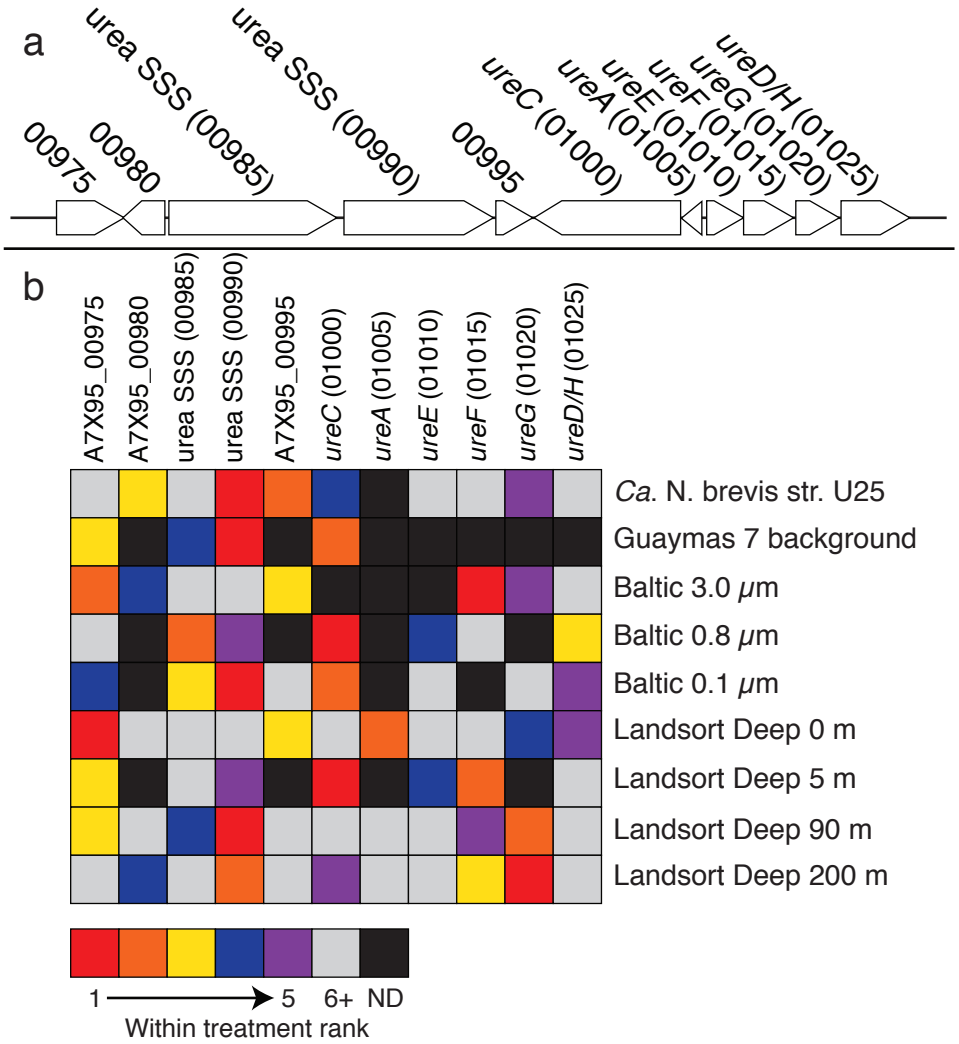

891

892 **Figure 1:** Urea transport and catalysis genes are frequently the most highly
893 expressed *Ca*. N. brevis U25-specific genes. (a) Chromosomal orientation
894 of the *Ca*. N. brevis str. U25 indel conferring urea transport and catalysis
895 capability. (b) Heatmap illustrating the relative rank expression level of the
896 five most abundant genes within the urea indel region for culture
897 experiments and environmental metatranscriptomes. Rank was calculated
898 within a given treatment from RPKM normalized expression values, where
899 a rank of 1 is the most abundant transcript of the genes contained in the
900 indel. The mean expression (n=3 replicates) value was used for ranking the
901 culture treatment. ND=Not detected. Note this is not the rank of the
902 transcript within the entire metatranscriptome. Some metatranscriptomes
903 were excluded because they did not have sufficient coverage of the urea
904 transport and catabolism machinery. Numbers in parentheses after gene
905 names refer to A7X95 locus tags.

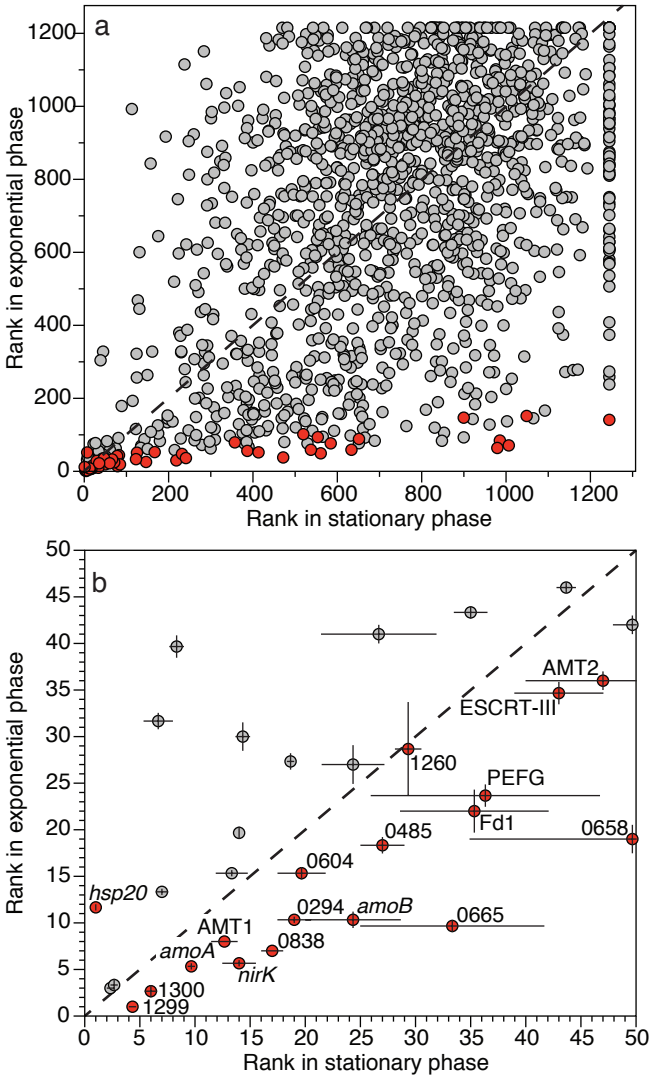

Figure 2: Highly expressed *Ca*. N. brevis str. CN25 transcripts in exponential phase are also highly expressed in stationary phase, despite significant differences in abundance. (a) Points are the mean rank (n=3) of RPKM normalized expression values for all genes in exponential and stationary growth phases. Red points are transcripts that were significantly differentially abundant across treatments (Supplementary Table 2). The abundances of grey points were not significantly different across treatments. Dashed line is 1:1 line indicating no change in rank. (b) Subset of panel (a), illustrating the rank of transcripts that are in the top 50 most abundant transcripts in both exponential and stationary phase. Points in (b) are the mean rank and error bars represent ± SE (n=3). Gene transcript abundances in (b) that were significantly different across treatments are labeled and colored red. The 'T478_' prefix is omitted from labels of genes annotated as 'hypothetical'. PEFG corresponds to T478_0596.

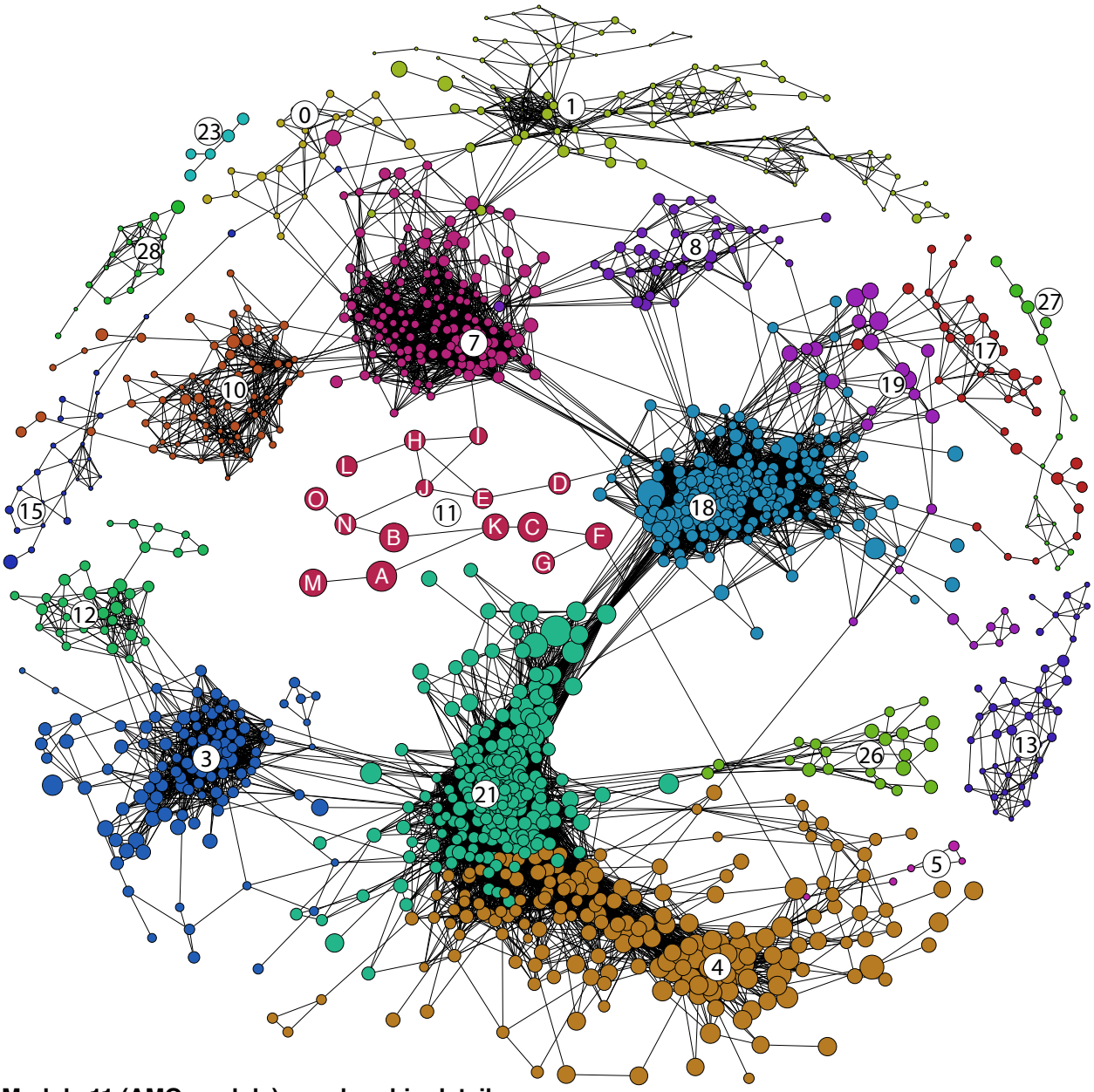

Module 11 (AMO module) membership details

A: *amoA* (0302)	I: ESCRT-III (0057)
B: *amoB* (0298)	J: PEFG-CTERM (0270)
C: *amoC* (0300)	K: *nirK* (1026)
D: Membrane-bound cupredoxin (0895)	L: *amoX* (0301)
E: 0487	M: AMT1 (1378)
F: Fd1 (1472)	N: Cupredoxin PEFG-CTERM (1362)
G: Fd2 (1259)	O: Fe-S cluster assembly protien (1056)
H: 1317	

Figure 3: Thaumarchaeal gene expression is highly modular and ammonia oxidation genes are co-expressed. Network diagram of strong and significant (Pearson's r ≥ 0.8, *q* value ≤ 0.025) positive correlations across ten environmental metatranscriptomes and the *Ca.* N. brevis U25

926 transcriptome depicted in Fig. 1 and a *Ca.* N. brevis CN25 transcriptome
927 from a culture initiated with 100 μM NH_4Cl (12 conditions total, see
928 methods). Individual nodes are genes. Nodes are sized by the mean
929 normalized rank abundance (VdW scores), whereby larger nodes are more
930 abundant transcripts on average. Nodes are colored by module
931 membership. Circled numbers are the module identity (Supplementary
932 Table 3). The module 11 (the AMO module) genes are identified by letters
933 A-O; their annotations are provided below network. Numbers in
934 parentheses refer to T478 locus tags. Only modules with five or more
935 nodes are shown for clarity; see Supplementary Table 3 for all module
936 membership details.
937

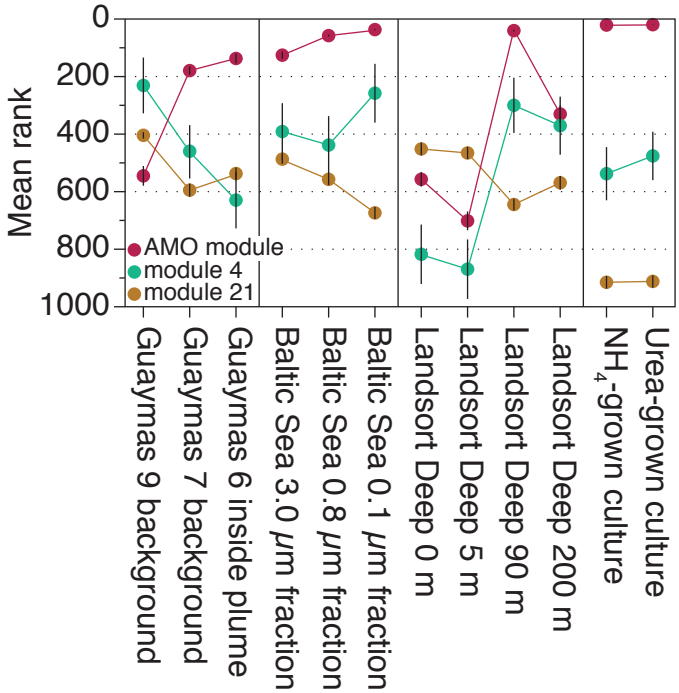

Fig. 4: Natural variability in the mean rank of expression modules across environments and culture conditions. Points are the average rank of all genes contained within a given module at each site; error bars are ± SE. On average, the AMO module and modules 36, 4 and 21 rank the highest (that is, they are the most abundant) across all sites. Module 36 is not displayed because it is only comprised of two genes, which prevents statistical analysis, and these genes are absent in the U25 genome.